Carrier mass measurements in degenerate indium nitride

G. Pettinari, A. Polimeni,* and M. Capizzi
Dipartimento di Fisica and CNISM, Sapienza Università di Roma, P.le A. Moro 2, 00185 Roma, Italy

J. H. Blokland, P. C. M. Christianen, and J. C. Maan
High Field Magnet Laboratory, Institute for Molecules and Materials, Radboud University Nijmegen, Toernooiveld 7, 6525 ED Nijmegen, The Netherlands

V. Lebedev, V. Cimalla, and O. Ambacher
Fraunhofer Institute for Applied Solid State Physics, Tullastr. 72, 79108 Freiburg, Germany
(Received 10 November 2008; revised manuscript received 18 March 2009; published 23 April 2009)

We present photoluminescence measurements under intense magnetic fields (B up to 30 T) in n-doped indium nitride samples with carrier concentration ranging from about 7.5×10^{17} cm^{-3} to 5×10^{18} cm^{-3}. The observation of transitions involving several Landau levels permits to determine the carrier-reduced mass μ around the Γ point. Depending on the carrier concentration, we find μ ranging between $0.093m_0$ and $0.107m_0$ (m_0 is the electron mass in vacuum). This finding poses a lower limit to the electron effective mass, whose unexpectedly large value ($m_e \geq 0.093m_0$) indicates that the sources of n doping in InN perturb strongly the crystal conduction band near its minimum.

DOI: 10.1103/PhysRevB.79.165207 PACS number(s): 78.55.Cr, 71.70.Di, 71.55.Eq, 71.20.Nr

I. INTRODUCTION

Indium nitride (InN) is widely investigated because of its potential in a variety of applications ranging from photovoltaics to fast and high-power electronics.[1–3] However, intrinsic indium nitride has not been obtained, yet, and as-grown InN samples have usually a free-electron concentration n_e in excess of 10^{17} cm^{-3}. This is one of the reasons why the value of the band-gap energy E_g has remained an elusive quantity for a long time and only few years ago it has been established that InN is—indeed—a small-gap semiconductor ($E_g \sim 0.65$ eV at room temperature[4,5]). Another fundamental—still not accurately determined—quantity is the electron effective mass m_e.

Until now, most of the m_e values reported have been inferred from infrared reflectivity[6–10] or ellipsometry[11–13] measurements aimed at determining the plasma resonance frequency $\omega_p^2=(n_e e^2)/(\langle m_e\rangle \varepsilon_0 \varepsilon_\infty)$, where ε_∞ is the high-frequency dielectric constant and $\langle m_e\rangle$ is the electron effective mass averaged over the density of states (DOS) of the conduction band.[11,14] ω_p depends explicitly on the average electron mass as well as on the carrier concentration, whose exact determination, however, is affected by the presence of a large sheet charge located at either the InN surface or at the interface between InN and its buffer layer.[15–17] In turn, this may influence the determination of the value of the electron mass. Specifically, $\langle m_e\rangle$ was found to increase sizably with doping level from $0.039m_0$ (for $n_e=1.8\times10^{17}$ cm^{-3}) to $0.25m_0$ (for $n_e=7\times10^{20}$ cm^{-3}), where m_0 is the electron mass in vacuum.[7,9,11]

In this work, we report on the observation of Landau levels (LLs) in degenerate InN as measured by magnetophotoluminescence (magneto-PL) in samples having different electron concentration $n_e \sim (7.5-50)\times10^{17}$ cm^{-3}. Up to four LL recombinations are observed that allows us to determine straightforwardly the carrier-reduced mass around the Γ point $\mu=(1/m_e+1/m_h)^{-1}=(0.093-0.107)m_0$, m_h being the hole effective mass. The unexpectedly large value ($m_e \geq 0.093m_0$) of the electron effective mass at $k\sim0$ in degenerate InN points toward a sizable distortion of the crystal conduction-band minimum caused by the sources of n-type doping.

II. EXPERIMENT

We investigated a 500-nm-thick InN sample grown by molecular-beam epitaxy on an epitaxial template formed by GaN(0001)/AlN/Al_2O_3. The narrow full width at half maximum of the sample rocking curves and a mobility value of about 1300–1500 cm^2/(V×s) indicate a good sample quality. The sheet carrier density derived by Hall-effect measurements is $n_H=1.2\times10^{14}$ cm^{-2} (assuming a uniform dopant distribution, this results in a volume concentration $n_H=2.4\times10^{18}$ cm^{-3}) that falls in the range reported by various authors.[6–9,11–13] Two pieces of the same sample were irradiated by a low-energy (10–20 eV) hydrogen-ion beam for different doses of impinging ions in order to achieve a controlled increase in the electron concentration, as reported recently in Ref. 18. Secondary ion mass spectrometry measurements on InN epilayers deuterated under the same experimental conditions employed in this work showed that the deuterium concentration profile is rather uniform over all the InN layer. PL was excited by the 532 nm line of a vanadate:Nd laser and detected by a liquid-nitrogen-cooled InGaAs photodiode coupled to a 0.25-m-long monochromator. Magneto-PL was performed in a 30 T water-cooled resistive magnet with the sample held at about 5 K (the spectra have been normalized by the optical set-up response).

III. RESULTS AND DISCUSSION

A. Degenerate GaAs

Not many previous reports on magneto-PL in degenerate bulk semiconductors exist. In fact, in these systems a free

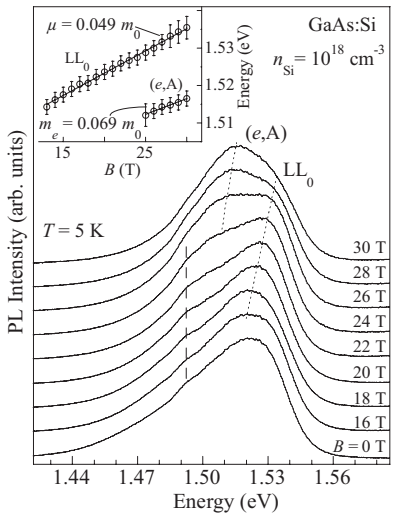

FIG. 1. Peak-normalized PL spectra of a reference GaAs sample heavily doped with Si (nominal impurity density equal to 10^{18} cm^{-3}). The spectra were recorded under different magnetic field intensities B at $T=5$ K, in steps of 1 T. A cooled InGaAs array detector and a 0.3-m-long monochromator were used for detection. LL_0 indicates the transition between the first Landau levels in the conduction and valence band. (e,A) indicates a free-electron to neutral-acceptor recombination. The dotted lines are guides for the eyes. The vertical dashed line indicates a spurious spectral feature due to the optical set-up response. Inset: dependence on magnetic field of the energy (open circles) of the transitions highlighted in the main part of the figure. The lines are fits to the data in terms of the Landau levels involved in the transitions considered. The best fit values of the free exciton reduced mass and electron effective mass are displayed.

carrier most likely undergoes several scattering events with other carriers and ionized impurities that could hamper the observation of Landau quantization and, consequently, affect the interpretation of the magneto-PL results. For this reason, we investigated first the effects of the magnetic field in heavily doped GaAs, whose fundamental properties (e.g., E_g and m_e) are well known. Figure 1 shows the magneto-PL spectra of a degenerate GaAs sample doped with Si impurities having nominal concentration equal to 10^{18} cm^{-3}. The PL spectrum results from the recombination of photoexcited and impurity-related free electrons in the conduction band and photoexcited holes in the valence band. The asymmetric PL line shape is characteristic of heavily doped semiconductors.[18] No change in the PL spectrum is observed up to $B=12$ T. For $B>12$ T, the PL peak blue shifts and a second lower-energy band is clearly detected for $B>24$ T. The peak energy of these two bands depends linearly on magnetic field with different slopes, as shown in the inset of Fig. 1. We ascribe the higher-energy component to an interband transition involving the $n=0$ electron and hole Landau levels (LL_0). Consequently, its energy depends on magnetic field as $E_{n=0}(B)=E(0)+\hbar eB/(2\mu)$. By using $\mu=(1/m_e+1/m_h)^{-1}$ and the zero-field band-gap energy $E(0)$ as free parameters, one obtains $\mu=(0.049\pm0.004)m_0$ and $E(0)=1.500$ eV. These values are in fairly good agreement, respectively, with the reduced mass of GaAs (0.057 m_0) (Ref. 19) and the renormalized band-gap energy in doped GaAs (1.495 eV) with $n_e=10^{18}$ cm^{-3}.[20,21] As for the lower-energy band appearing for $B>24$ T, the corresponding B-induced shift gives $\mu=(0.069\pm0.002)m_0$ and an extrapolated transition energy at $B=0$ T equal to 1.490 eV. These values are close, respectively, to the electron effective mass and to the energy of the acceptor-related recombination (e,A) bands in GaAs. As a result, the lower-energy band is attributed to a free-electron to neutral-acceptor transition, whose shift with magnetic field is known to reproduce that of the lowest LL of electrons ($\mu\rightarrow m_e$).[22,23] The (e,A) transition dominates the PL spectrum at high fields likely because the increasing magnetic field leads to an enhanced overlap between the free electron and localized hole wave functions (and increased PL intensity). Such an intensity enhancement induced by B should be sizably smaller for the uncorrelated electron-hole pairs involved in the LL_0 transition. In turn, this accounts for the relative variation in the intensity of the (e,A) and LL_0 bands with varying B. As mentioned, no Landau-level quantization is observed until $B>12$ T thus providing a rough estimation of the carrier scattering time $\tau=1/\omega_c=m_e/(e\cdot 12\ \mathrm{T})=30$ fs, a value falling in the range of those reported for heavily doped GaAs.[24]

To conclude this part, we can state that magneto-PL can be properly used to derive the carrier mass in a highly degenerate bulk semiconductor.

B. Degenerate InN

We now consider the effect of magnetic field on indium nitride. A magneto-PL study has been recently performed in disordered InN samples characterized by a broad PL symmetric line shape (linewidth in excess of 90 meV) and a low carrier mobility (<200 cm^2/Vs).[25] In particular, in Ref. 25, the dominating presence of localized states in the PL spectra did not permit to study the effects of magnetic field on delocalized carriers in degenerate InN. Indeed, at about 50 T, only a very small diamagnetic shift (~2.5 meV) could be observed.[25] On the contrary, the InN samples considered here exhibit a recombination band with an asymmetric line shape characteristic of degenerate semiconductors (PL linewidth ranging from 30 to 82 meV). Figure 2 shows the magneto-PL spectra at $T\sim 5$ K of InN samples both untreated (as-grown) and H irradiated with dose $d_H=1z$ and $d_H=2z$, where z corresponds to 1×10^{15} ions/cm^2. Upon hydrogen incorporation, the high-energy edge and the maximum of the PL spectrum both shift at high energy (see bottommost curves in Fig. 2). This is a consequence of the donor nature of hydrogen in InN that leads to a large controllable increase in the free-electron concentration.[18] In all samples, no sizable variation in the PL line shape is detected for $B<16$ T likely due to carrier scattering effects, as discussed before for GaAs. Although the sources of scattering in InN are different from those in heavily doped GaAs, the lowest field before LLs are observable is similar in the two materials, thus indicating that scattering influences carrier motion to a similar extent. In as-grown InN, the PL peak blue shifts by about 10 meV when $B=30$ T. Concomitantly, the full width at half maximum of the recombination band decreases from 32 to 22 meV as a consequence of the B-induced increase in the crys-

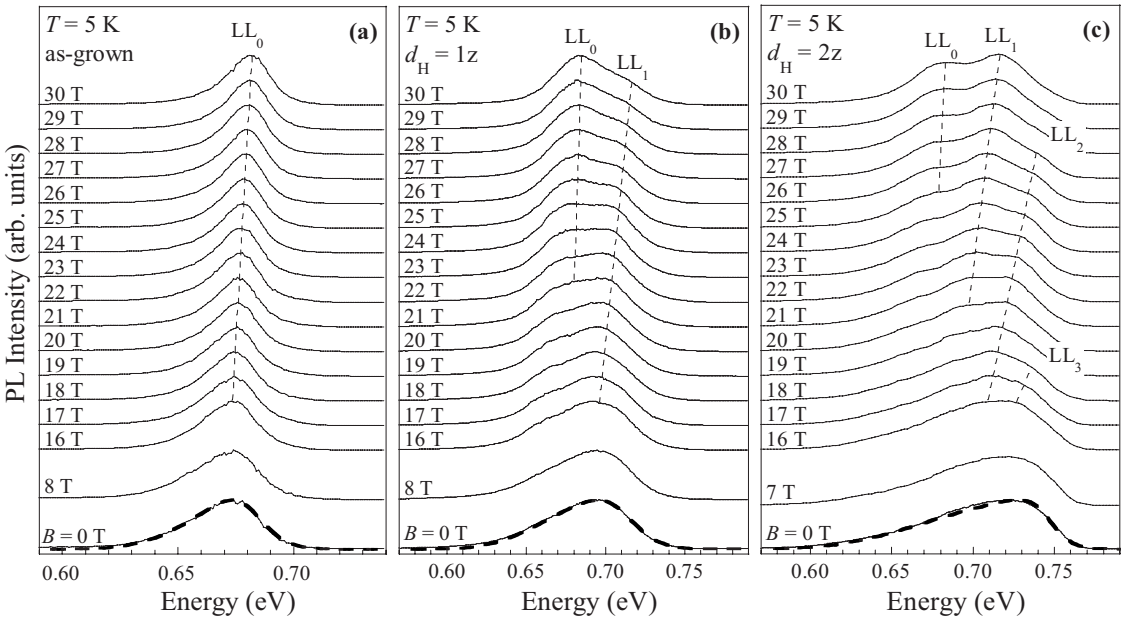

FIG. 2. Peak-normalized PL spectra of InN samples irradiated with different H doses d_H: (a) untreated (as-grown), (b) hydrogenated ($d_H=1z$), and (c) hydrogenated ($d_H=2z$), where $z=1\times10^{15}$ cm^{-2}. The spectra were recorded at $T=5$ K for different magnetic field values, in steps of 1 T. LL_n indicates a transition between the nth Landau levels in the conduction and valence band. The dotted lines are guides for the eyes. The dashed thick lines superimposed on the $B=0$ T spectra are simulations to the data via the Kane's model (see Ref. 18).

tal density of states.[26] In the hydrogenated samples (where the electron density is greater), several PL bands appear as B increases. In particular, the bands at high-energy lose spectral weight in favor of low-energy bands, which dominate the spectrum at the highest B. The peaks of the different components move with magnetic field at a quite different pace; in particular, the high-energy lying components are much faster than those at low energy. This field dependence points toward transitions related to Landau levels with different index n,

$$E_n(B) = E(0) + \left(n + \frac{1}{2}\right)\frac{\hbar eB}{\mu}. \quad (1)$$

It should be noted that the greater number of LLs visible in hydrogenated samples is a direct consequence of the larger density of free electrons available in those samples. In addition, with increasing B, the LL degeneracy increases ($\propto B$) and more carriers can occupy the lower index LLs, thus determining a progressive depopulation of higher index levels, as shown in Fig. 2. The thick dashed lines superimposed on the zero-field spectra of Fig. 2 are a simulation of the PL data by the semiclassical model developed by Kane and detailed in Ref. 18. We will give details on the parameters employed in the line-shape simulation in the following.

Before proceeding with a quantitative analysis of the data shown in Fig. 2, it is worth discussing further the appropriateness of using magneto-PL data to derive the electron effective mass in InN. Indium nitride is a small-gap semiconductor and, therefore, it is more subject to nonparabolicity effects than, e.g., GaAs. As a matter of fact, previous ellipsometry and reflectivity measurements showed a marked dependence of $\langle m_e \rangle$ on carrier concentration,[27] indicating a nonconstant value of the electron effective mass over the conduction-band dispersion curve. However, the shift of the Landau levels with magnetic field measured by magneto-PL is mainly determined by the value of the carrier-reduced mass at the Γ point of the InN conduction and valence bands. Indeed, as the magnetic field is turned on, the change in the dimensionality of the carrier motion from three-dimensional(3D) to one-dimensional(1D) like implies a change in the energy dependence of the crystal DOS (Refs. 28 and 29): a much larger carrier occupancy at the band extrema is expected for 1D (DOS$\propto 1/\sqrt{E}$) than for 3D (DOS$\propto\sqrt{E}$). Hence, the peak of the PL bands shown in Fig. 2 can be attributed to carriers recombining mainly at $k\sim0$ in the respective LL and the slope of the emission-peak energy with B is ultimately determined by the carrier mass at the conduction-band minimum and valence-band maximum. It is worth mentioning that magneto-optical measurements were performed on different small-gap semiconductors, such as InAs and InSb, and it was proved that the Landau theory may be applied using the effective-mass approximation.[30]

Figure 3 summarizes the dependence on magnetic field of the peak energy of all the observed recombination bands (symbols) in untreated as well as H-irradiated samples. Lines are fits to the data by Eq. (1) with different n's, using μ and $E(0)$ as free parameters. For all samples, we find $E(0)=(0.664\pm0.001)$eV, while we derive $\mu=(0.093\pm0.001)m_0$ in the untreated sample, $\mu=(0.106\pm0.002)m_0$ in the sample hydrogenated with $d_H=1z$ and $\mu=(0.107\pm0.002)m_0$ in the sample hydrogenated with $d_H=2z$. Nonparabolicity effects on the conduction band can be estimated using the approach described in Ref. 31. In our case, assuming a negligible contribution from valence-band nonparabolicity, we obtain a similarly good fit with the same band-gap energy at $B=0$ T and reduced masses about 10% smaller than those

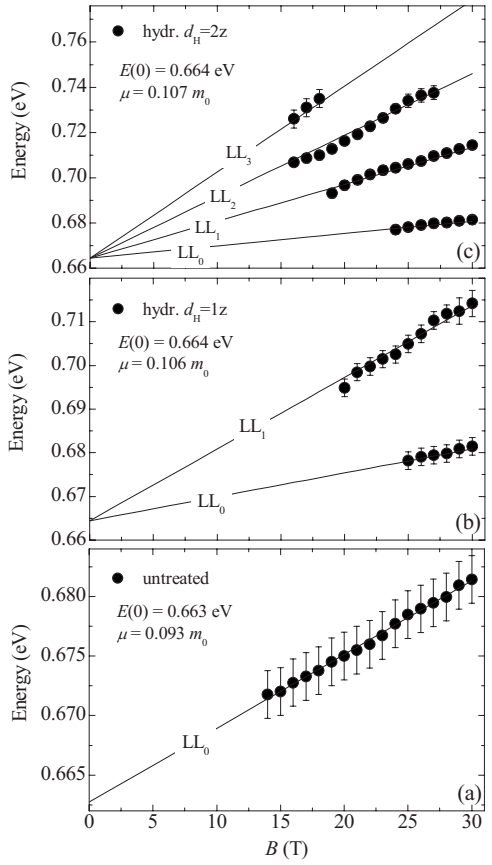

FIG. 3. Energies of the LL$_n$ transitions highlighted in Fig. 2 as a function of the magnetic field. (a) refers to the untreated (as-grown) sample. (b) and (c) refer, respectively, to samples hydrogenated with $d_H=1z$ and $d_H=2z$ ($z=10^{15}$ cm^{-2}). Lines are fits to the data by Eq. (1), where the value of the band-gap energy at $B=0$ T, $E(0)$, and the value of the carrier reduced mass μ are used as fit parameters for each sample separately.

derived directly by Eq. (1). However, data scattering (likely due to the relatively broad PL linewidth) does not allow us to discriminate which model describes better the experimental data.

In order to extract the electron effective mass from μ, one should know the value of the hole effective mass m_h. Unfortunately, no direct estimation of m_h exists and, therefore, we can only give a lower bound for the electron mass $m_e \geq 0.093m_0$. It should be mentioned that some authors interpreted low-temperature PL spectra in InN as mainly (or partly) due to a free-electron to neutral-acceptor transition.[32–34] Within this picture, the values of μ here derived would coincide with the electron effective mass.[22,23] However, the dependences of the PL spectra on temperature and laser excitation density do not give any hint that the PL band we observe is due to an electron-acceptor transition. In the limiting case of $m_e=\mu$, one may obtain an estimation of the electron carrier concentration in the samples by simulating the PL spectra at $B=0$ T by the Kane's model,[18] as shown by the thick dashed lines in Fig. 2. One finds n_e equal to 7.5×10^{17} cm^{-3}, 2.1×10^{18} cm^{-3}, and 4.7×10^{18} cm^{-3}, in the order, for as-grown InN and samples hydrogenated with the lower and the higher H dose.[35] In the untreated sample, the carrier-concentration value derived from PL line-shape analysis is sizably smaller than the value found from Hall measurements (see Sec. II). As mentioned, this is likely due to a charge accumulation at the sample interfaces.[15–17] This charge should not influence PL results. In fact, the contribution to PL from photogenerated carriers at the surface and/or InN/buffer interface is negligible due to the presence of large electric fields and/or dead layer effects arising from surface nonradiative centers.[36] In addition, the relatively narrow linewidth of the PL spectrum of the as-grown sample points toward a constant background electron concentration over the sample volume probed by radiatively recombining carriers.

We now compare our electron mass lower limit with the $\langle m_e \rangle$ values obtained by infrared reflectivity or ellipsometry measurements reported in the literature.[6–11,13] Those measurements provide the density-of-states-averaged electron mass from $k=0$ to the Fermi wave vector k_F,[11,14] whose value depends on the doping level of the samples. In that case, the $k=0$ limit can be deduced for $n_e \to 0$ that corresponds to an *ideally intrinsic* InN and gives $m_e \sim 0.05-0.07m_0$.[7,9,27] Here, instead, we determine the electron effective mass mainly at Γ point ($m_e \gtrsim 0.1m_0$) in a *really doped* ($n_e \gtrsim 10^{18}$ cm^{-3}) InN sample. Therefore, the large discrepancy found between the two types of measurements ought to be due to doping in indium nitride. We speculate that in InN, the nature of *n*-type dopants perturbs the host crystal to a quite large extent (contrary to what is observed in degenerate GaAs). Among the proposed sources of doping are nitrogen vacancies and/or antisites and incorporation of oxygen and hydrogen atoms.[18,37,38] Although to a different extent, these donor sources may disorder the lattice potential thus giving rise to an enhanced localized character (and increased effective mass) of the conduction-band minimum then possibly accounting for the increase in the carrier-reduced mass observed in the hydrogen-irradiated samples. Alternatively, a contribution to the PL spectra from $k \neq 0$ states characterized by the higher conduction-band curvature may result in a reduced Landau-level shift and, hence, in an averaged larger carrier mass.

IV. CONCLUSIONS

In conclusion, we presented carrier mass measurements in heavily doped bulk semiconductors (GaAs and InN) by magnetophotoluminescence up to $B=30$ T. In both systems, high magnetic fields (12 T and 16 T for GaAs and InN, respectively) are necessary to overcome decoherence of the carrier cyclotron orbit induced by carrier and/or donor scattering. In InN, we observe Landau-level interband recombinations, whose number increases with the sample free-electron concentration. This latter has been purposely varied from about 7.5×10^{17} cm^{-3} to 4.7×10^{18} cm^{-3} by postgrowth H irradiation. By the slope of the Landau levels, we determine the carrier-reduced mass at the Γ point: $\mu=(0.093\pm0.002)m_0$ in the untreated InN sample ($n_e \sim 7.5\times10^{17}$ cm^{-3}) and $\mu=(0.106\pm0.002)m_0$ in the hydrogenated samples ($n_e \sim 2-5\times10^{18}$ cm^{-3}). Due to a lack of knowledge of the hole mass, we can only set a lower limit to the electron mass equal to

$0.093m_0$ in the H-free sample. This high mass at the conduction-band minimum can be justified by the strong k-space distortion caused by the crystal defects that are a source of doping in indium nitride.

ACKNOWLEDGMENTS

Part of this work has been supported by EuroMagNET through EU under Contract No. RII3-CT-2004-506239.

*antonio.polimeni@roma1.infn.it

[1] H. Lu, W. J. Shaff, J. Hwang, H. Wu, G. Koley, and L. F. Eastman, Appl. Phys. Lett. **79**, 1489 (2001).
[2] Y.-C. Kong, Y. D. Zheng, C. H. Zhou, Y. Z. Deng, B. Shen, S. L. Gu, R. Zhang, P. Han, R. L. Jiang, and Y. Shi, Solid-State Electron. **49**, 199 (2005).
[3] V. M. Polyakov and F. Schwierz, Appl. Phys. Lett. **88**, 032101 (2006).
[4] V. Yu. Davydov, A. A. Klochikhin, V. V. Emtsev, S. V. Ivanov, V. V. Vekshin, B. Bechstedt, J. Furthmüller, H. Harima, A. V. Mudryi, A. Hashimoto, J. Aderhold, J. Graul, and E. E. Haller, Phys. Status Solidi B **229**, r1 (2002).
[5] J. Wu, W. Walukiewicz, K. M. Yu, J. W. Ager III, E. E. Haller, H. Lu, W. J. Schaff, Y. Saito, and Y. Nanishi, Appl. Phys. Lett. **80**, 3967 (2002).
[6] T. Inushima, K. Fukui, H. Lu, and W. J. Schaff, Appl. Phys. Lett. **92**, 171905 (2008).
[7] S. P. Fu and Y. F. Chen, Appl. Phys. Lett. **85**, 1523 (2004).
[8] T. Inushima, M. Higashiwaki, and T. Matsui, Phys. Rev. B **68**, 235204 (2003).
[9] J. Wu, W. Walukiewicz, W. Shan, K. M. Yu, J. W. Ager, E. E. Haller, H. Lu, and W. J. Schaff, Phys. Rev. B **66**, 201403(R) (2002).
[10] T. Inushima, T. Shiraishi, and V. Y. Davydov, Solid State Commun. **110**, 491 (1999).
[11] P. Schley, C. Napierala, R. Goldhahn, G. Gobsch, J. Schörmann, D. J. As, K. Lischka, M. Feneberg, K. Thonke, F. Fuchs, and F. Bechstedt, Phys. Status Solidi C **5**, 2342 (2008).
[12] T. Hofmann, T. Chavdarov, V. Darakchieva, H. Lu, W. J. Schaff, and M. Schubert, Phys. Status Solidi C **3**, 1854 (2006).
[13] A. Kasic, M. Schubert, Y. Saito, Y. Nanishi, and G. Wagner, Phys. Rev. B **65**, 115206 (2002).
[14] L. R. Bailey, T. D. Veal, P. D. C. King, C. F. McConville, J. Pereiro, J. Grandal, M. A. Sánchez-Garcìa, E. Muñoz, and E. Calleja, J. Appl. Phys. **104**, 113716 (2008).
[15] V. Cimalla, V. Lebedev, F. M. Morales, R. Goldhahn, and O. Ambacher, Appl. Phys. Lett. **89**, 172109 (2006).
[16] C. S. Gallinat, G. Koblmüller, J. S. Brown, S. Bernardis, J. S. Speck, G. D. Chern, E. D. Readinger, H. Shen, and M. Wraback, Appl. Phys. Lett. **89**, 032109 (2006).
[17] P. D. C. King, T. D. Veal, and C. F. McConville, Phys. Rev. B **77**, 125305 (2008).
[18] G. Pettinari, F. Masia, M. Capizzi, A. Polimeni, M. Losurdo, G. Bruno, T. H. Kim, S. Choi, A. Brown, V. Lebedev, V. Cimalla, and O. Ambacher, Phys. Rev. B **77**, 125207 (2008).
[19] S. Shokhovets, O. Ambacher, and G. Gobsch, Phys. Rev. B **76**, 125203 (2007).
[20] J. Shah, R. F. Leheny, and W. Wiegmann, Phys. Rev. B **16**, 1577 (1977).
[21] G. Tränkle, H. Leier, A. Forchel, H. Haug, C. Ell, and G. Weimann, Phys. Rev. Lett. **58**, 419 (1987).
[22] J. A. Rossi, C. M. Wolfe, and J. O. Dimmock, Phys. Rev. Lett. **25**, 1614 (1970).
[23] F. Masia, G. Pettinari, A. Polimeni, M. Felici, A. Miriametro, M. Capizzi, A. Lindsay, S. B. Healy, E. P. O'Reilly, A. Cristofoli, G. Bais, M. Piccin, S. Rubini, F. Martelli, A. Franciosi, P. J. Klar, K. Volz, and W. Stolz, Phys. Rev. B **73**, 073201 (2006).
[24] Z. G. Hu, M. B. M. Rinzan, S. G. Matsik, A. G. U. Perera, G. Von Winckel, A. Stintz, and S. Krishna, J. Appl. Phys. **97**, 093529 (2005).
[25] B. Bansal, A. Kadir, A. Bhattacharya, and V. V. Moshchalkov, Appl. Phys. Lett. **93**, 021113 (2008).
[26] D. Bimberg, Phys. Rev. B **18**, 1794 (1978).
[27] I. Gorczyca, J. Plesiewicz, L. Dmowski, T. Suski, N. E. Christianen, A. Svane, C. S. Gallinat, G. Koblmueller, and J. S. Speck, J. Appl. Phys. **104**, 013704 (2008).
[28] R. W. J. Hollering, T. T. J. M. Berendschot, H. J. A. Bluyssen, H. A. J. M. Reinen, P. Wyder, and F. Roozeboom, Phys. Rev. B **38**, 13323 (1988).
[29] W. Rühle and E. Göbel, Phys. Status Solidi B **78**, 311-317 (1976).
[30] S. Zwerdling, B. Lax, and L. M. Roth, Phys. Rev. **108**, 1402 (1957).
[31] D. C. Tsui, Phys. Rev. B **12**, 5739 (1975).
[32] B. Arnaudov, T. Paskova, P. P. Paskov, B. Magnusson, E. Valcheva, B. Monemar, H. Lu, W. J. Schaff, H. Amano, and I. Akasaki, Phys. Rev. B **69**, 115216 (2004).
[33] M. Feneberg, J. Däubler, K. Thonke, R. Sauer, P. Schley, and R. Goldhahn, Phys. Rev. B **77**, 245207 (2008).
[34] A. A. Klochikhin, V. Yu. Davydov, V. V. Emtsev, A. V. Sakharov, V. A. Kapitonov, B. A. Andreev, H. Lu, and W. J. Schaff, Phys. Rev. B **71**, 195207 (2005).
[35] The parameters entering into the simulation are the band-gap energy (E_g), the electron mass, and the electron density (n_e). The static dielectric constant was kept equal to $\varepsilon_r = 10.5\ \varepsilon_0$ (see Ref. 8) and the hole mass equal to $m_h = 0.42m_0$ [X. Wang, S.-B. Che, Y. Ishitani, and A. Yoshikawa, Appl. Phys. Lett. **92**, 132108 (2008)]. The electron mass values employed are those derived by the analysis of the magnetic field data presented in Fig. 3. The band-gap energy too is equal (=0.642 eV) for all samples.
[36] G. F. Brown, J. W. Ager III, W. Walukiewicz, W. J. Schaff, and J. Wu, Appl. Phys. Lett. **93**, 262105 (2008).
[37] A. Janotti and C. G. Van de Walle, Appl. Phys. Lett. **92**, 032104 (2008).
[38] C. G. Van de Walle and J. Neugebauer, J. Appl. Phys. **95**, 3851 (2004).